Supporting Information for

On the Origins of the Salt-Concentration-Dependent Instability and Lateral Nanoscale Heterogeneities of Weak Polyelectrolyte Brushes: Gradient Brush Experiment, and Flory-Type Theoretical Analysis

Jaehyun Hur, Kevin N. Witte, Wei Sun, and You-Yeon Won*

School of Chemical Engineering, Purdue University, West Lafayette, Indiana 47907

* To whom correspondence should be addressed. E-mail: yywon@ecn.purdue.edu

Figure S1. (A) The chemical structure of poly(2-(dimethylamino)ethyl methacrylate)-poly(*n*-butyl acrylate) (PDMAEMA-PnBA) diblock copolymer; the PDMAEMA and PnBA blocks are denoted in red and brown, respectively. (B) Schematic depiction of a Langmuir monolayer of PDMAEMA-PnBA, used as a model system for studies of the structure and phase behavior of weak polyelectrolyte brushes.

(A)

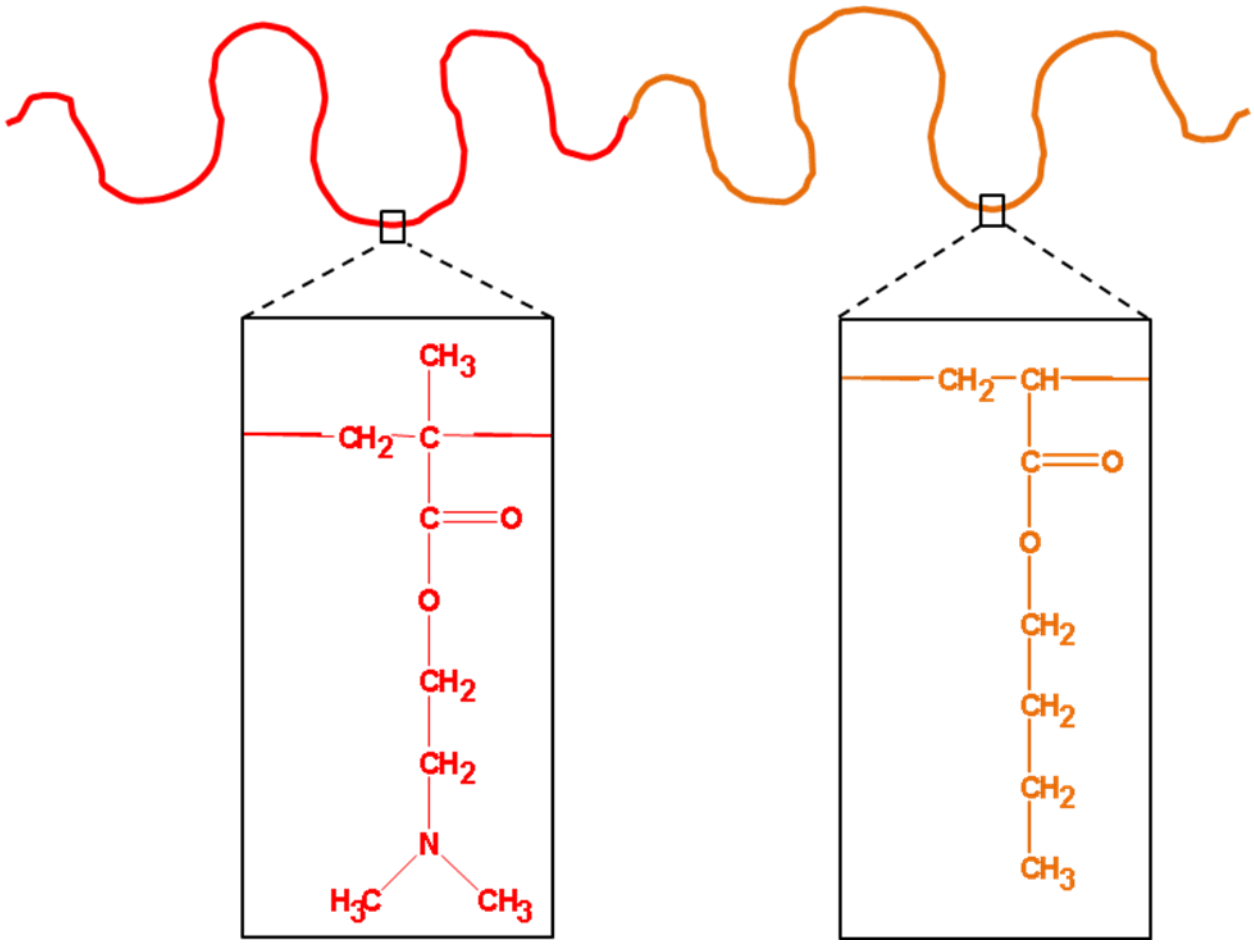

(B)

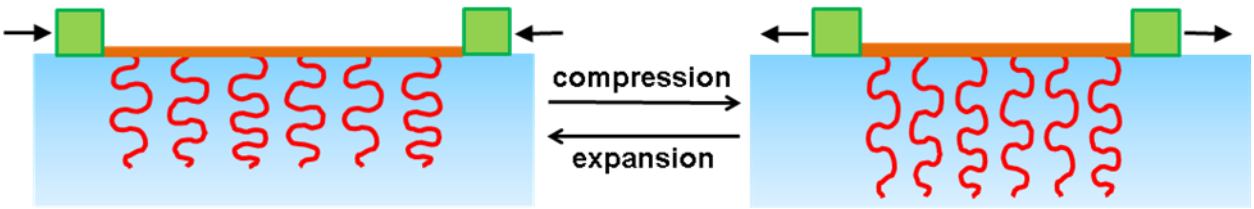

Figure S2. Representative fluid AFM tapping-mode height images (2 μm × 2 μm) and cross-sectional height profiles (along arbitrary horizontal (blue) and vertical (red) planes) of PDMAEMA brushes prepared by regular Langmuir-Blodgett techniques; the PnBA-PDMAEMA block copolymers were LB-deposited (at a deposition speed of 1.0 mm/min) onto atomically flat graphite surfaces under no salt and neutral pH conditions at various monolayer areas: $1/\sigma$ = (A) 1943, (B) 1650, (C) 1357, (D) 1064 and (E) 770 $Å^2$/chain (i.e., LB-deposited brush samples, each having a uniform grafting density, were prepared separately at various grafting densities). For each sample, AFM imaging was performed within 1 day after the preparation. Part (A) of this figure has been reproduced from the data presented in Figure 3(C) of Reference 27.

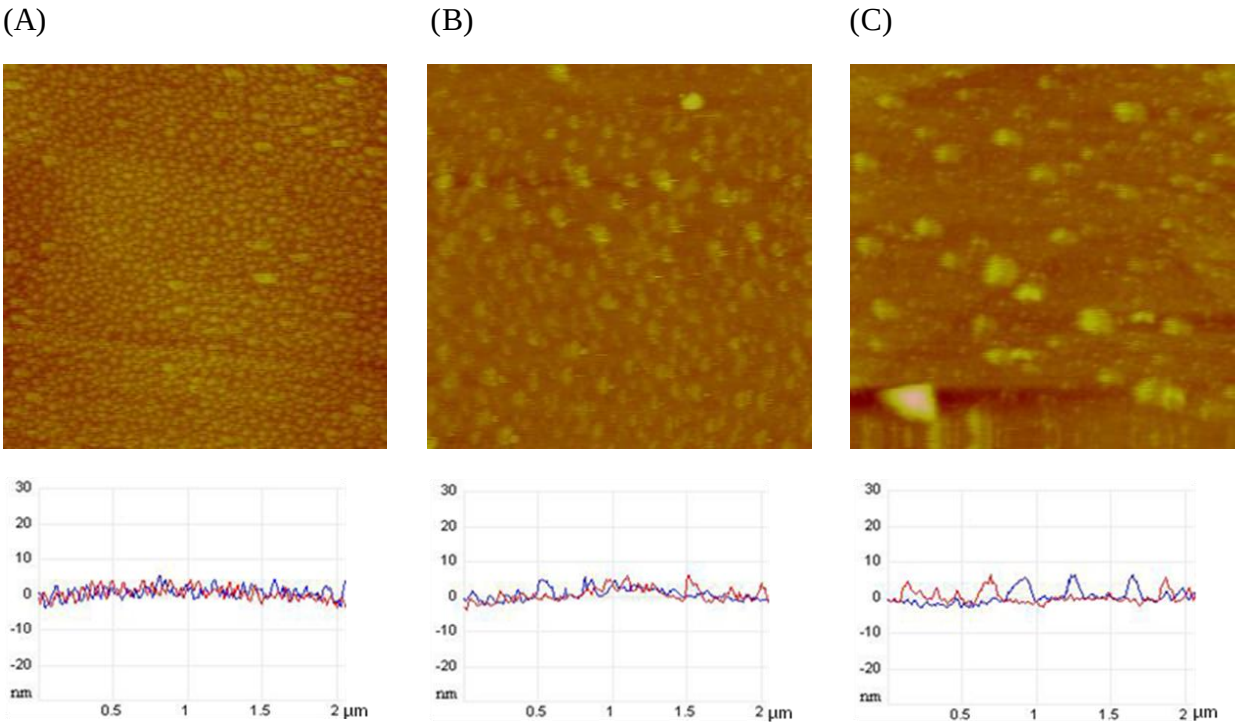

(D)

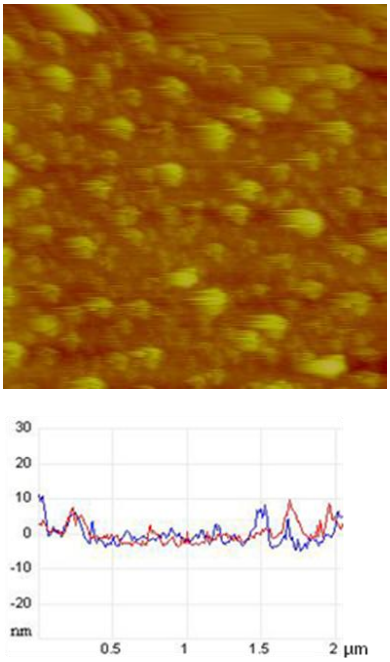

(E)

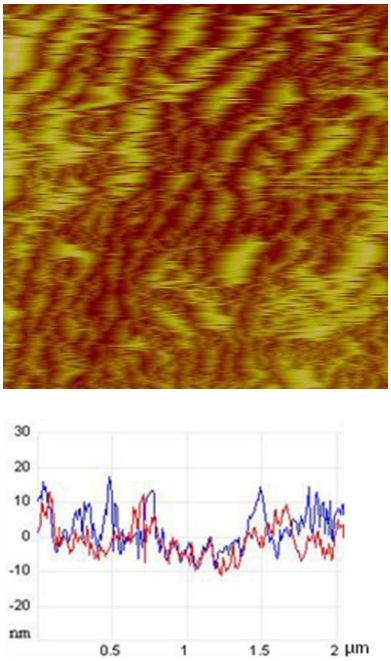

Figure S3. Representative fluid AFM tapping-mode height images (2 μm × 2 μm) and cross-sectional height profiles (along arbitrary horizontal (blue) and vertical (red) planes) obtained from a PDMAEMA brush sample in which the grafting density varies continuously from one end of the sample to the other. This gradient brush sample was prepared by using the LB\C technique; a Langmuir monolayer of PDMAEMA-PnBA was LB-transferred at a rate of 1.0 mm/min onto a graphite surface in DI water (0 mM NaCl, pH 7), and during this process, the PDMAEMA-PnBA monolayer at the air-water interface was compressed at a rate of 5.0 mm/min from an initial monolayer area of 1943 $Å^2$/chain to a final area of 842 $Å^2$/chain. The AFM measurements were carried out about 24 hours after the preparation of the sample. AFM images were taken from 4 different positions in the gradient brush specimen: i.e., at (A) 0.0 ± 0.1, (B) 1.5 ± 0.1, (C) 3.0 ± 0.1 and (D) 4.5 ± 0.1 mm distance from the leading front of the brush layer, which correspond to area per chain values of $1/\sigma$ = (A) 1943 ± 24, (B) 1577 ± 24, (C) 1210 ± 24 and (D) 842 ± 24 $Å^2$/chain, respectively.

(A) (B)

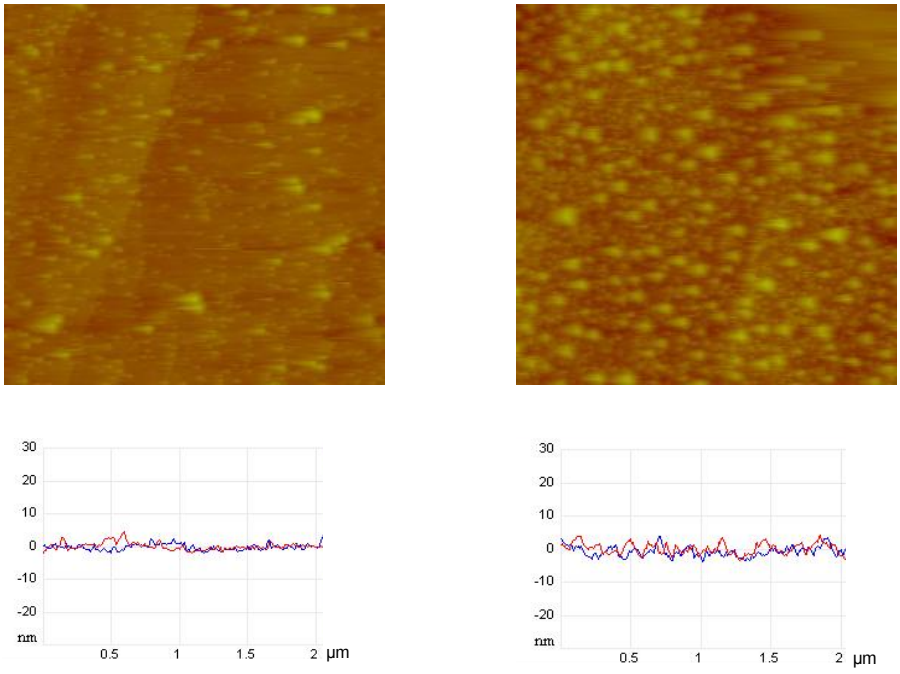

(C)

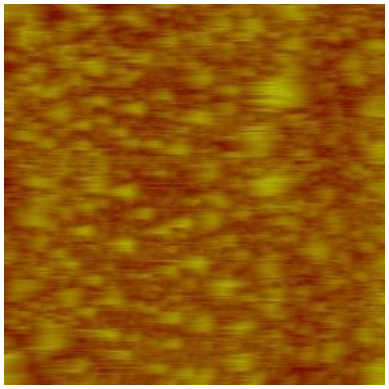

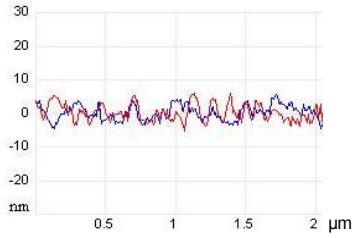

(D)

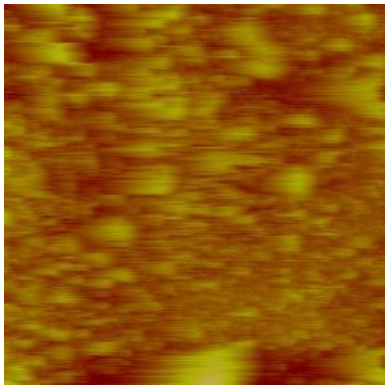

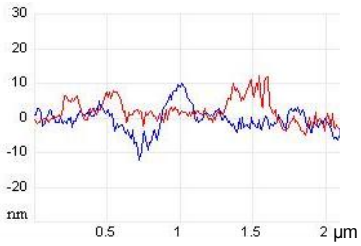

Figure S4. Representative fluid AFM tapping-mode height images (2 μm × 2 μm) and cross-sectional height profiles (along arbitrary horizontal (blue) and vertical (red) planes) obtained from a gradient PDMAEMA brush sample prepared using the same LB\C procedure as in the case demonstrated in Figure S5. In the present case, however, the AFM measurements were conducted at 2 weeks after the preparation of the sample. AFM images were taken from 5 different positions in the gradient brush specimen: i.e., at (A) 0.0 ± 0.1, (B) 1.2 ± 0.1, (C) 2.4 ± 0.1, (D) 3.6 ± 0.1 and (E) 4.8 ± 0.1 mm distance from the leading front of the brush layer, which correspond to area per chain values of $1/\sigma$ = (A) 1942 ± 24, (B) 1650 ± 24, (C) 1357 ± 24, (D) 1064 ± 24 and (E) 770 ± 24 $Å^2$/chain, respectively.

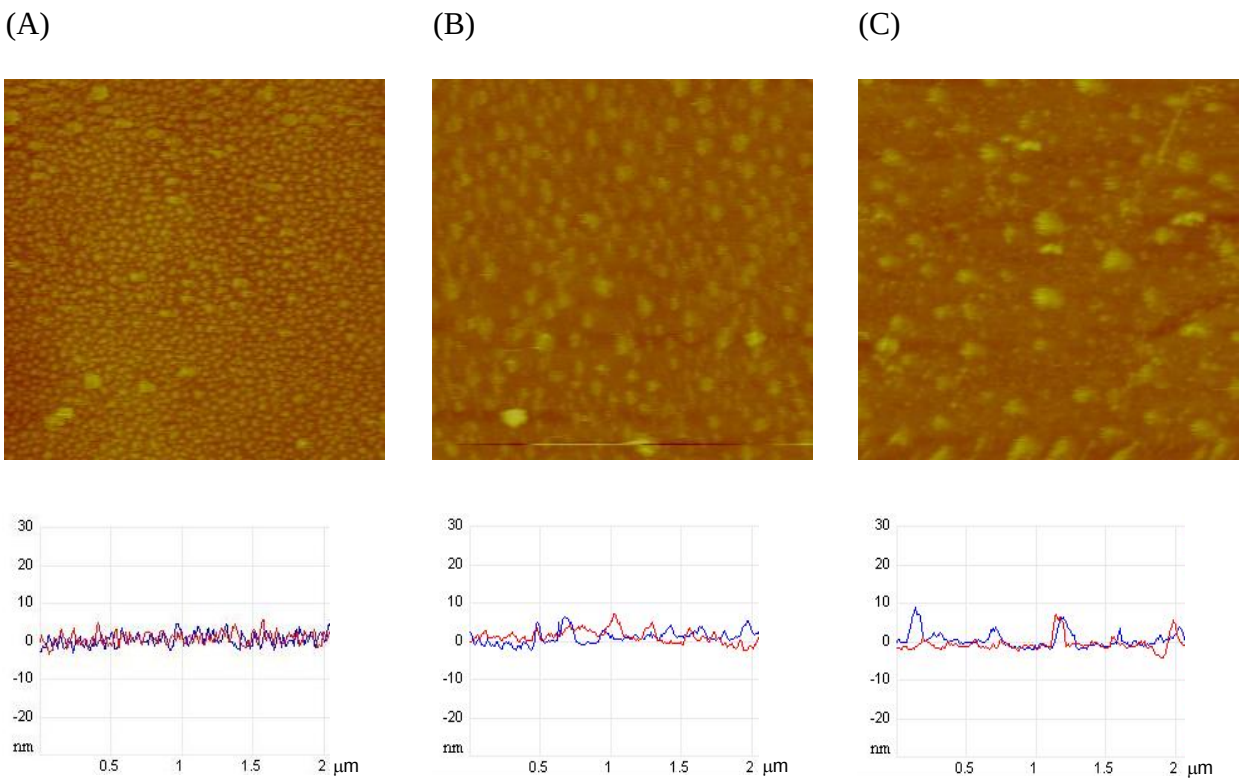

(D)

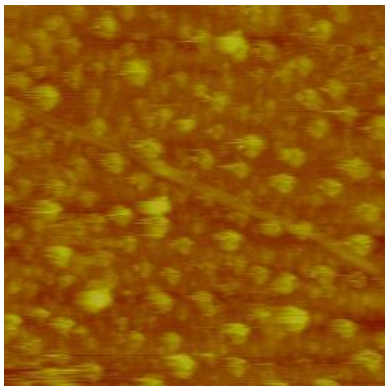

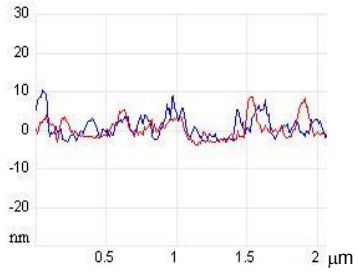

(E)

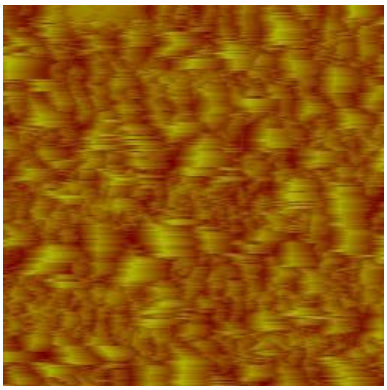

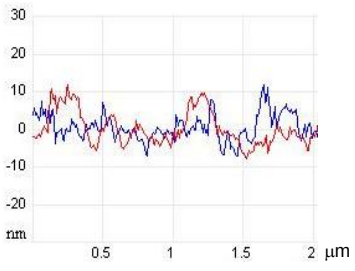

Figure S5. Comparison of the average widths (circles) and heights (squares) of the heterogeneities of the PDMAEMA brushes prepared by (i) the normal LB method (blue) and (ii) the LB\C technique (red); here, the heterogeneity width is defined as the distance between two adjacent peaks, and the heterogeneity height is defined as the peak-to-base distance. See Figures S2 and S4 for respective representative AFM images used in the analyses. For calculation of these average quantities, sufficient numbers of heterogeneous objects were used (with minimum N = 220 per analysis). The error bars represent the standard deviations of the means.

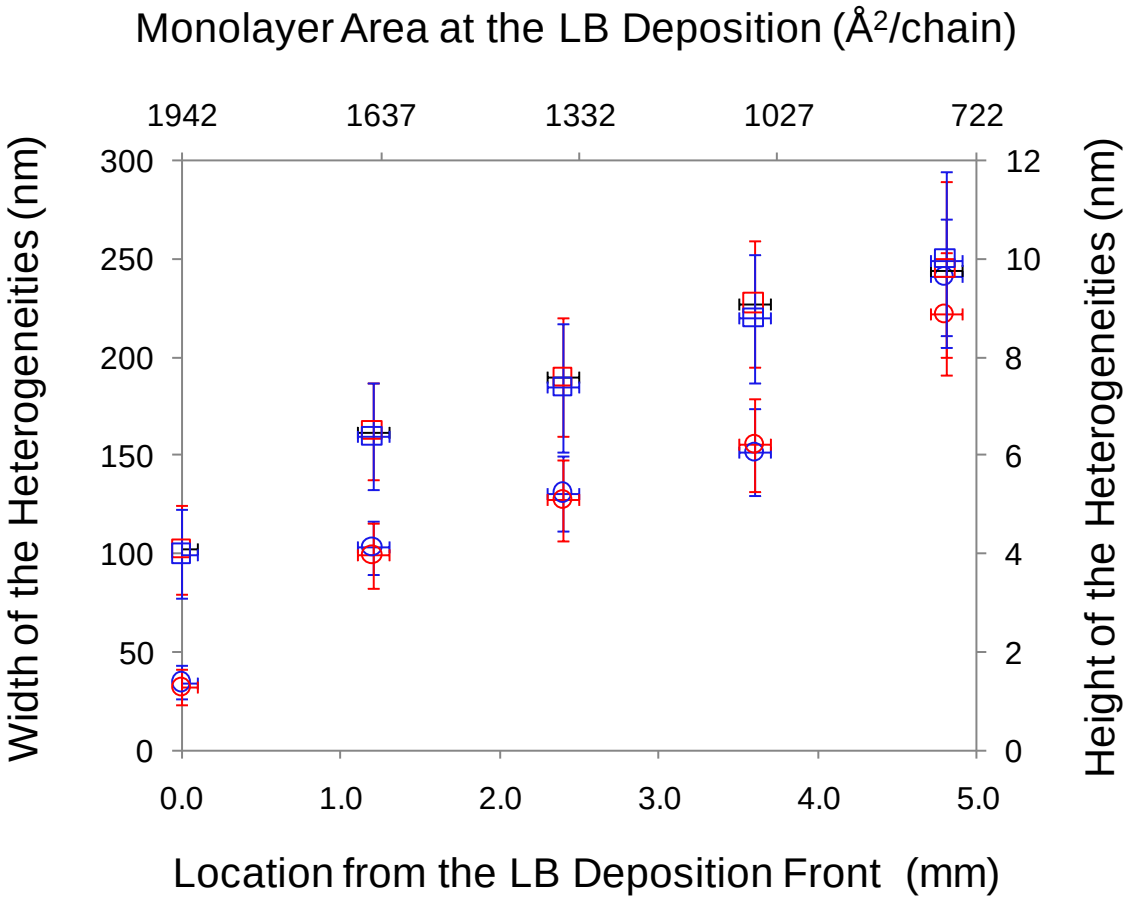

Figure S6. Representative fluid AFM tapping-mode height images (2μm × 2μm) of PDMAEMA brushes with *no added salt* under pH 7 at five different inverse grafting densities of $1/\sigma$ = (A) 1942 ± 24, (B) 1650 ± 24, (C) 1357 ± 24, (D) 1064 ± 24 and (E) 770 ± 24 $Å^2$/chain. The PDMAEMA brush sample was prepared by using the LB\C method; a Langmuir monolayer of PDMAEMA-PnBA was LB-transferred at a rate of 1.0 mm/min onto a graphite surface in DI water (0 mM NaCl, pH 7) over a five-minute period, and during this process, the PDMAEMA-PnBA monolayer at the air-water interface was compressed at a rate of 5.0 mm/min from an initial monolayer area of 1942 $Å^2$/chain to a final area of 719 $Å^2$/chain. The AFM measurements were carried out about 24 hours after the preparation of the sample. AFM images were taken from 5 different positions in the gradient brush specimen: i.e., at (A) 0.0 ± 0.1, (B) 1.2 ± 0.1, (C) 2.4 ± 0.1, (D) 3.6 ± 0.1 and (E) 4.8 ± 0.1 mm distance from the leading front of the brush layer, which correspond to the above respective area per chain ($1/\sigma$) values.

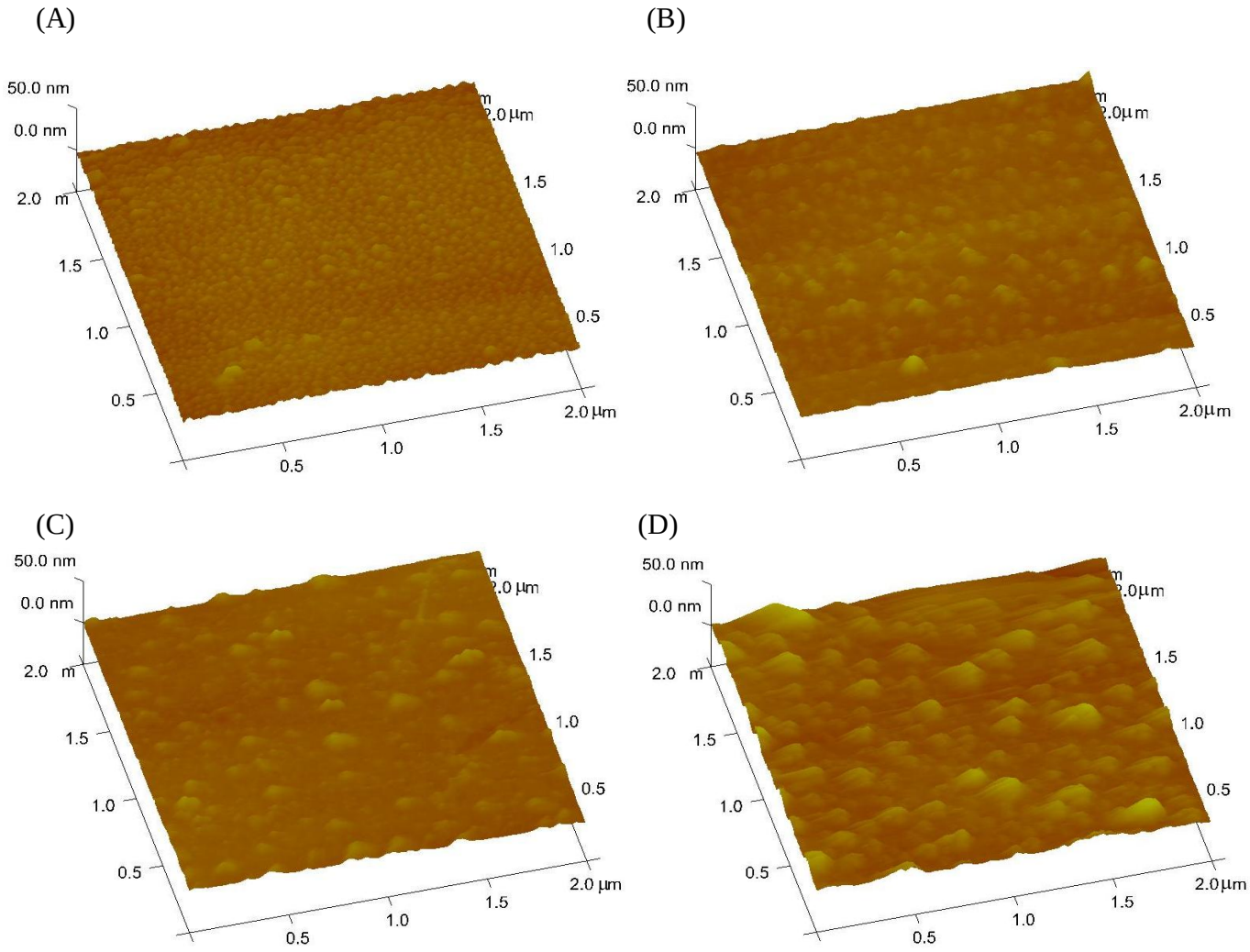

(E)

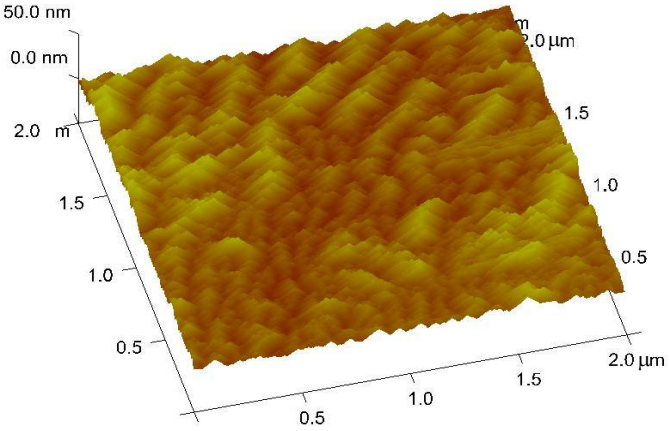

Figure S7. Representative fluid AFM tapping-mode height images (2μm × 2μm) of the PDMAEMA brushes with added *60 mM NaCl* under pH 7 at five different inverse grafting densities of $1/\sigma$ = (A) 1942 ± 24, (B) 1650 ± 24, (C) 1357 ± 24, (D) 1064 ± 24 and (E) 770 ± 24 $Å^2$/chain. The PDMAEMA brush sample was prepared by using the LB\C method.

(A)

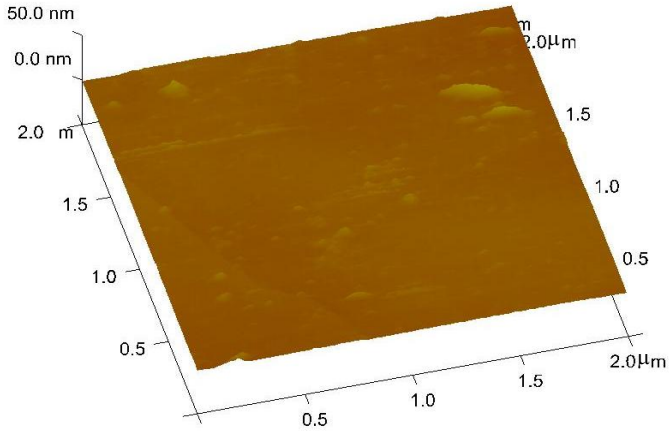

(B)

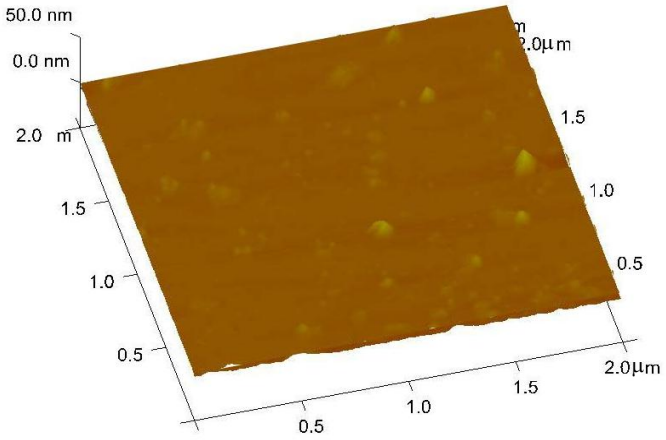

(C)

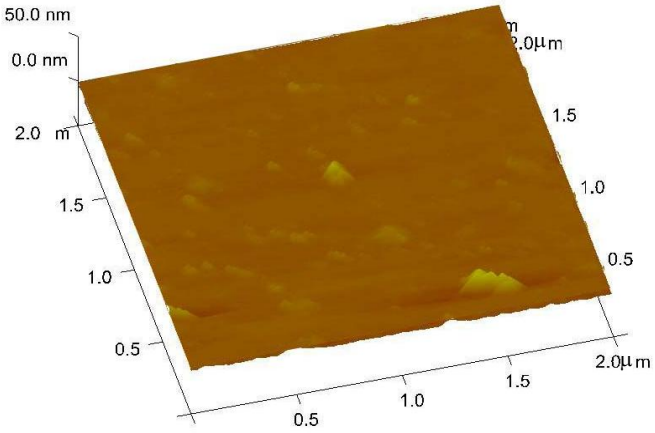

(D)

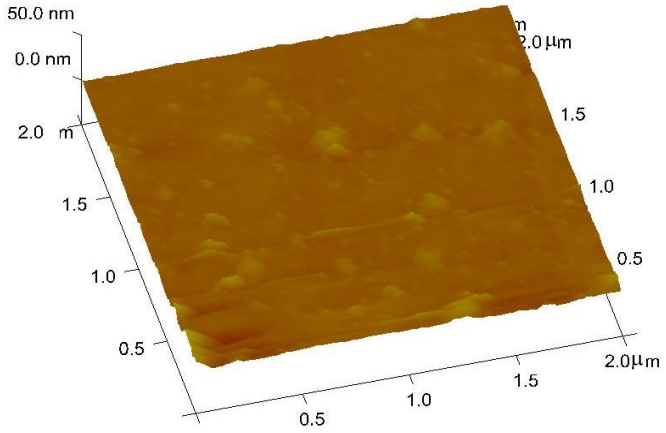

(E)

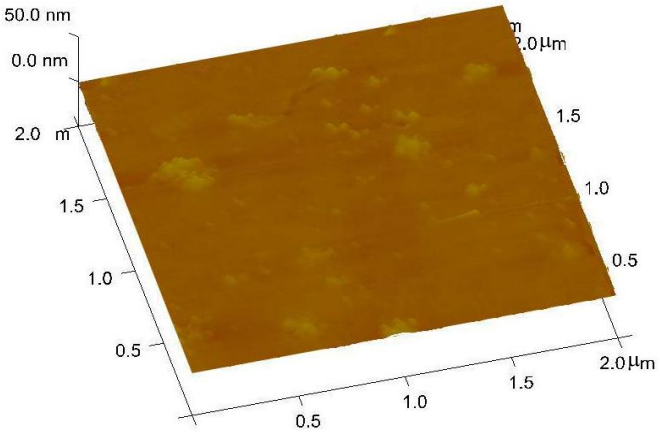

Figure S8. Representative fluid AFM tapping-mode height images (2μm × 2μm) of the PDMAEMA brushes with added *100 mM NaCl* under pH 7 at five different inverse grafting densities of $1/\sigma$ = (A) 3887, (b) 2591, (c) 1943, (d) 1296 and (e) 648 $Å^2$/chain. Each sample was prepared separately by the normal LB technique at the respective $1/\sigma$ values.

(A)

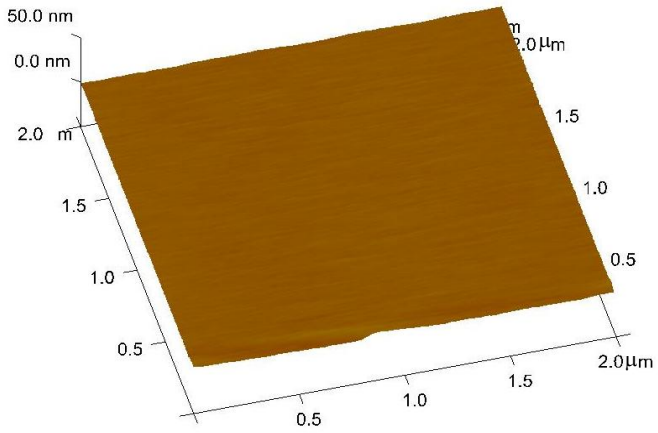

(B)

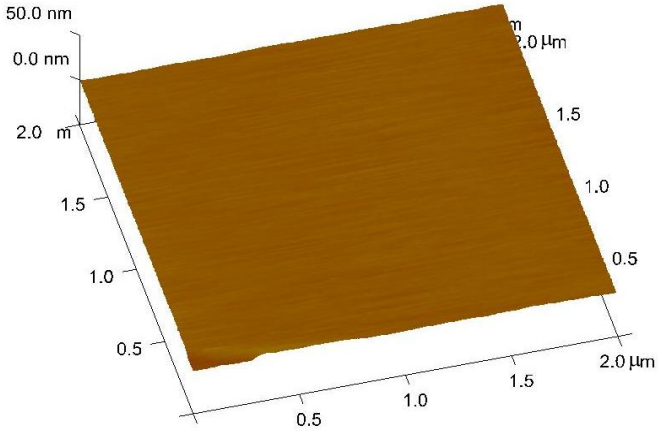

(C)

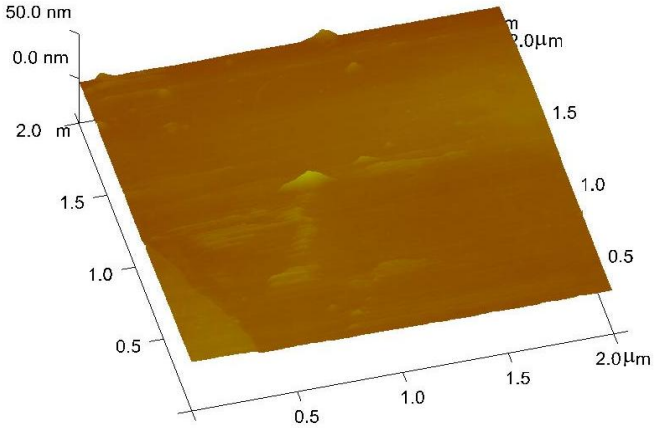

(D)

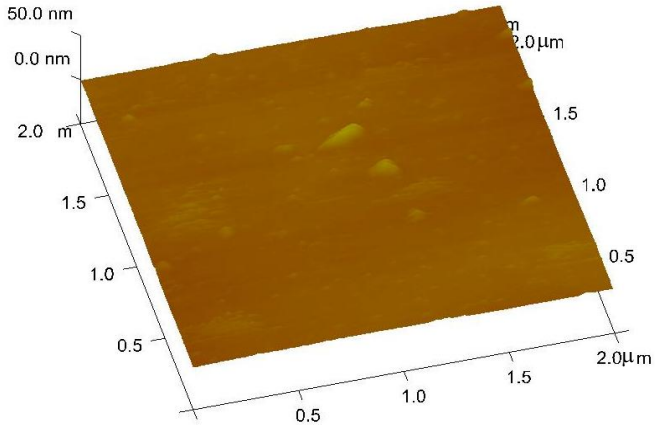

(E)

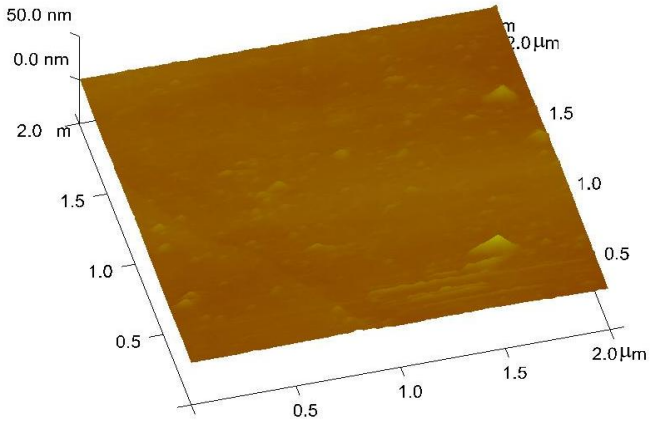

Figure S9. Representative fluid AFM tapping-mode height images (2μm × 2μm) of the PDMAEMA brushes with added *300 mM NaCl* under pH 7 at five different inverse grafting densities of $1/\sigma$ = (A) 1942 ± 24, (B) 1650 ± 24, (C) 1357 ± 24, (D) 1064 ± 24 and (E) 770 ± 24 $Å^2$/chain. The PDMAEMA brush sample was prepared by using the LB\C method.

(A)

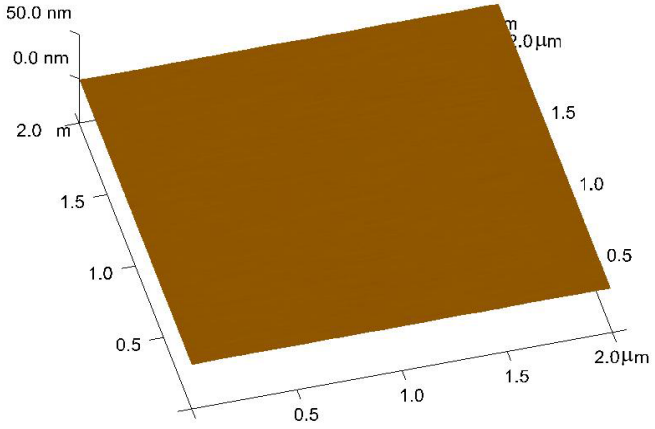

(B)

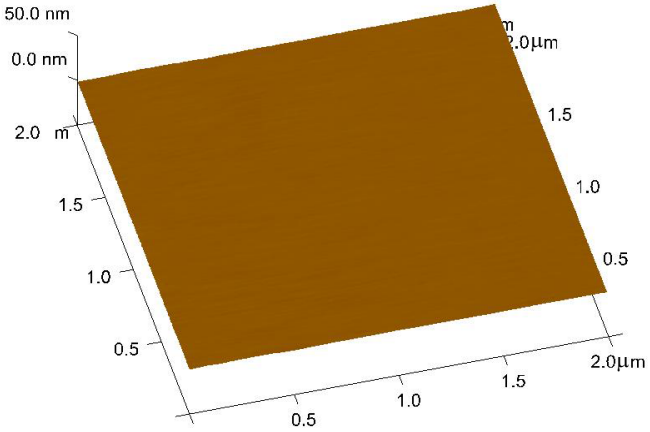

(C)

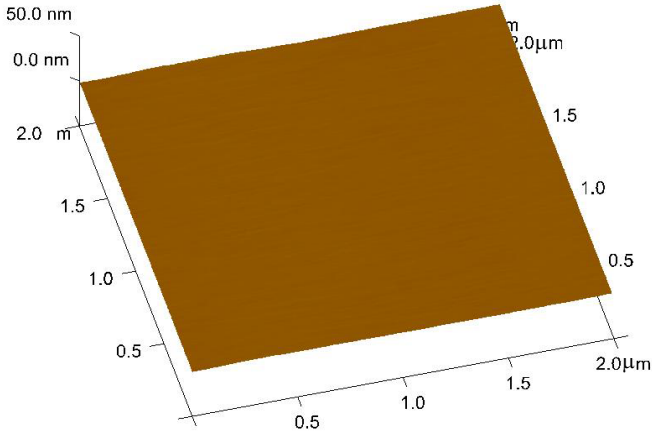

(D)

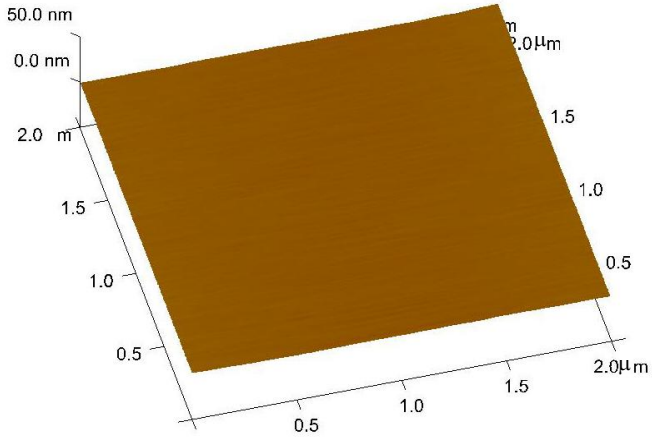

(E)

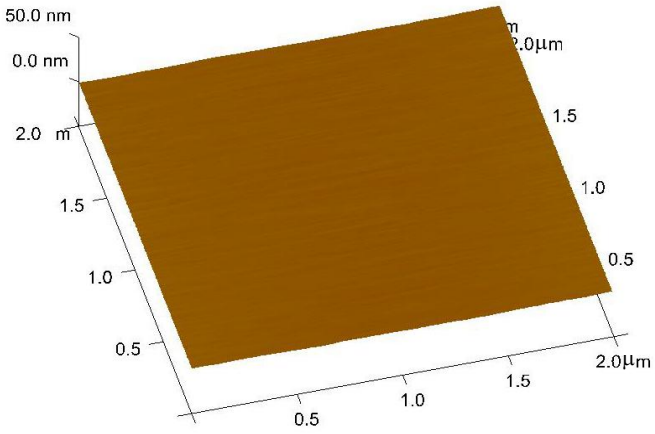

Figure S10. Plots of the osmotic free energy (F_{osm}) vs. scaled brush height (H/b, where b denotes the monomer size), estimated using Equation (1), at three different added NaCl concentrations of C_{Na^+} (= C_{Cl^-}) = (A) 60, (B) 100 and (C) 300 mM, representing two of the three different regimes of weak polyelectrolyte brush behavior discussed in the main text. The parameter values used are N = 100 (chain length), b = 7 Å (monomer size), v = -50 Å^3 (excluded volume), w = 10^4 Å^6 (three-body interaction coefficient), $C_{H_3O^+}$ = 10^{-7} M (bulk hydronium ion concentration), K = $10^{8.4}$ M^{-1} (protonation equilibrium coefficient), and $\sigma = 3/Nb^2$ (grafting density).

(A)

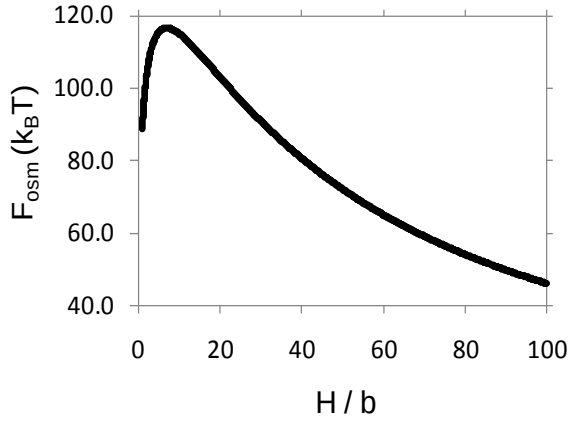

(B)

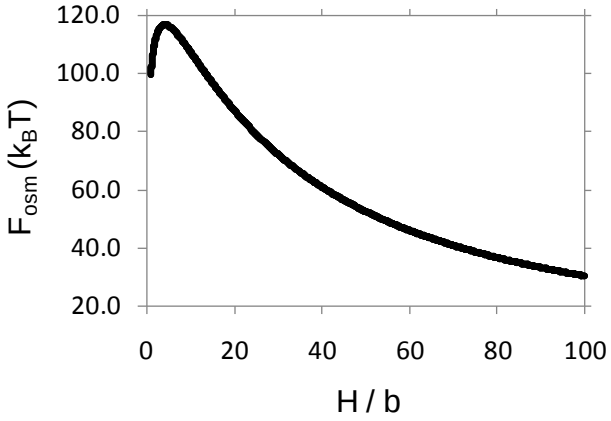

(C)

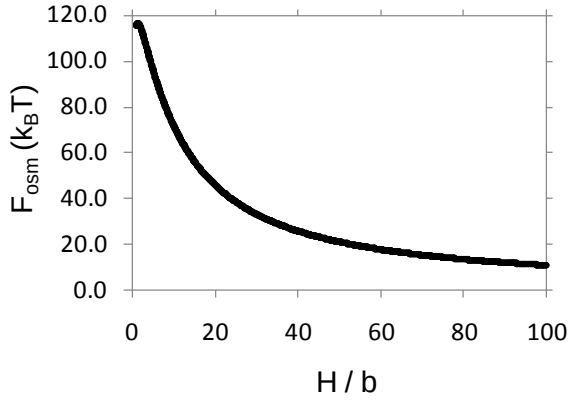

Figure S11. Plots of the polyelectrolyte chemical potential (μ) as a function of σNb^2, calculated according to Equation (8), at three different added NaCl concentrations of C_{Na^+} (= C_{Cl^-}) = (A) 60, (B) 100 and (C) 300 mM, representing two of the three different regimes of weak polyelectrolyte brush behavior discussed in the main text. For each salt condition, the effects of the three different (i.e., poor, θ and good) solvent-quality conditions were evaluated, respectively, at v = -50 (solid curve), 0 (dotted-broken curve) and 50 (broken curve) Å^3. The other parameter values used are N = 100 (chain length), b = 7 Å (monomer size), w = 10^4 Å^6 (three-body interaction coefficient), $C_{H_3O^+}$ = 10^{-7} M (bulk hydronium ion concentration), and K = $10^{8.4}$ M^{-1} (protonation equilibrium coefficient).

(A)

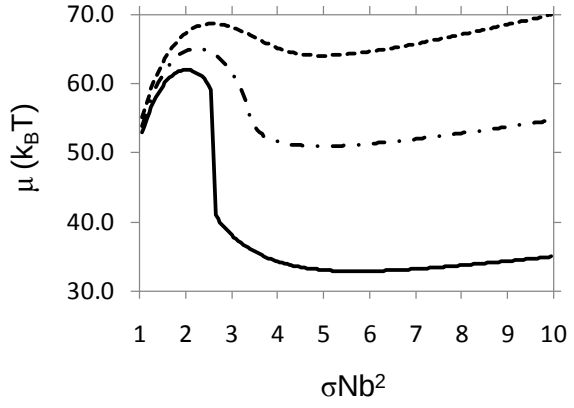

(B)

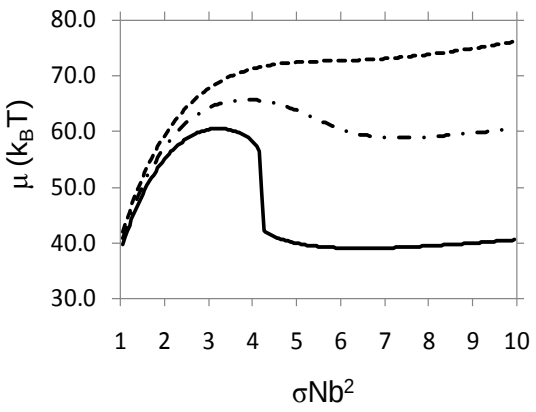

(C)

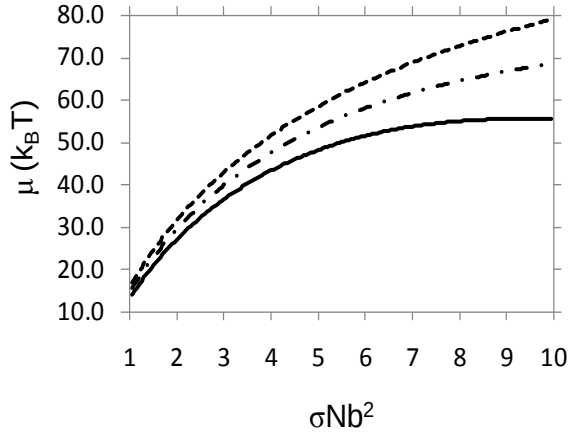

Figure S12. Plots of the polyelectrolyte chemical potential (μ) as a function of σ for strong (or quenched) polyelectrolyte brushes, calculated according to Equation (8) with three different fixed values of the fraction of charged monomers (f = 0.05, 0.10 and 0.50), under seven different salt conditions, i.e., (A) 0, (B) 20, (C) 60, (D) 80, (E) 100, (F) 300 and (G) 500 mM NaCl. The parameter values used are N = 100 (chain length), b = 7 Å (monomer size), v = -50 Å^3 (excluded volume), $w = 10^4$ Å^6 (three-body interaction coefficient), $C_{H_3O^+} = 10^{-7}$ M (bulk hydronium ion concentration), and $\sigma = 3Nb^2$ (grafting density). Note that here the polyelectrolyte is assumed to be hydrophobic (i.e., $v < 0$).

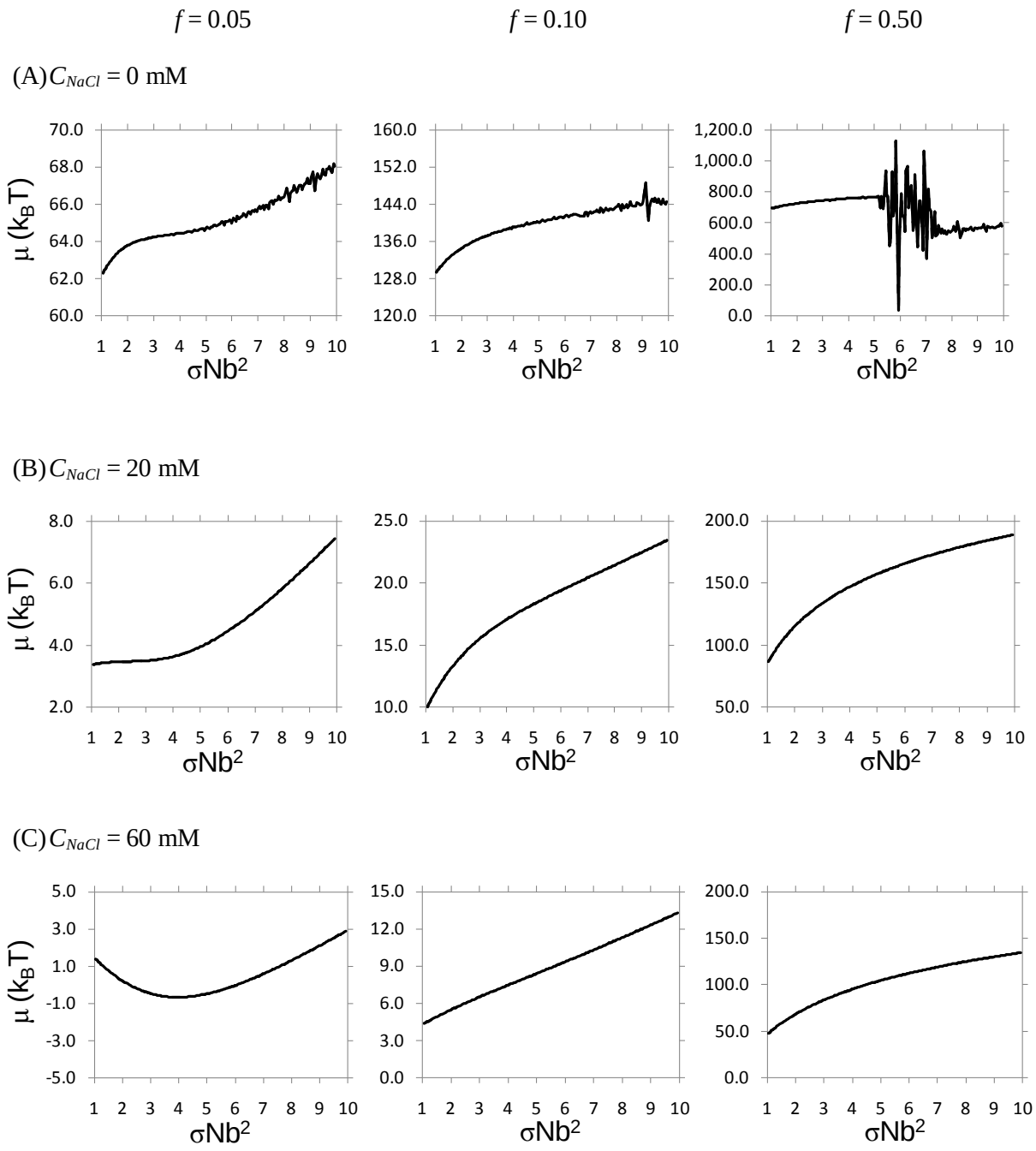

(D) C_{NaCl} = 80 mM

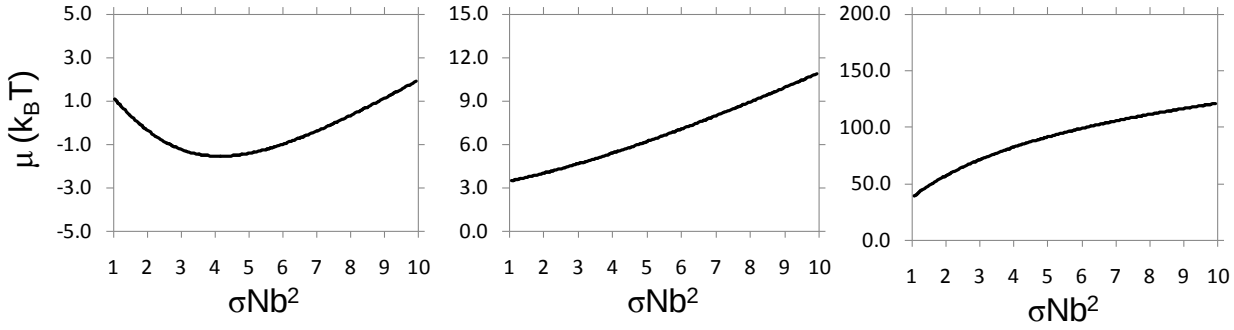

(E) C_{NaCl} = 100 mM

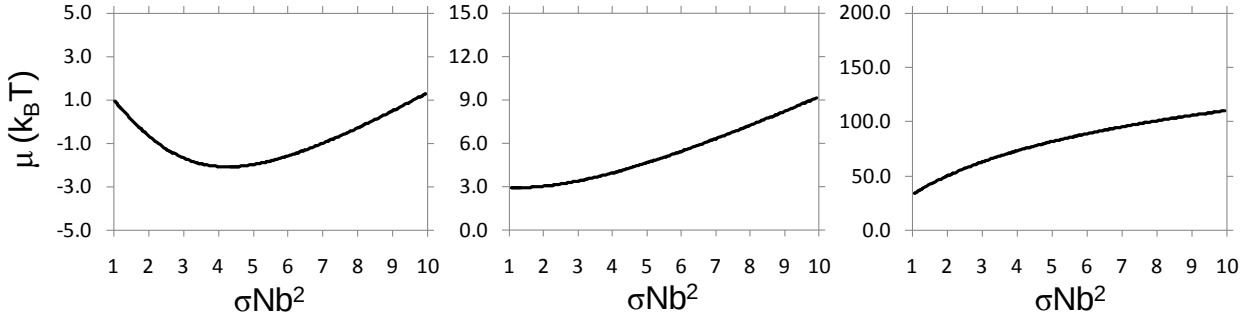

(F) C_{NaCl} = 300 mM

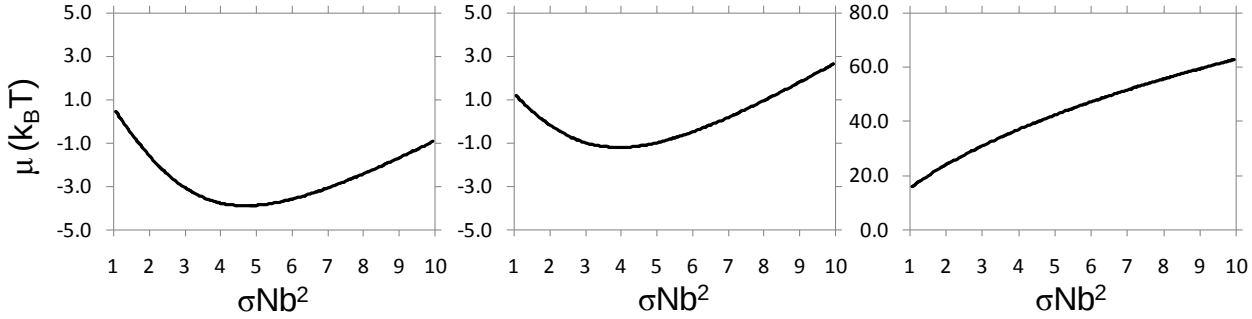

(G) C_{NaCl} = 500 mM

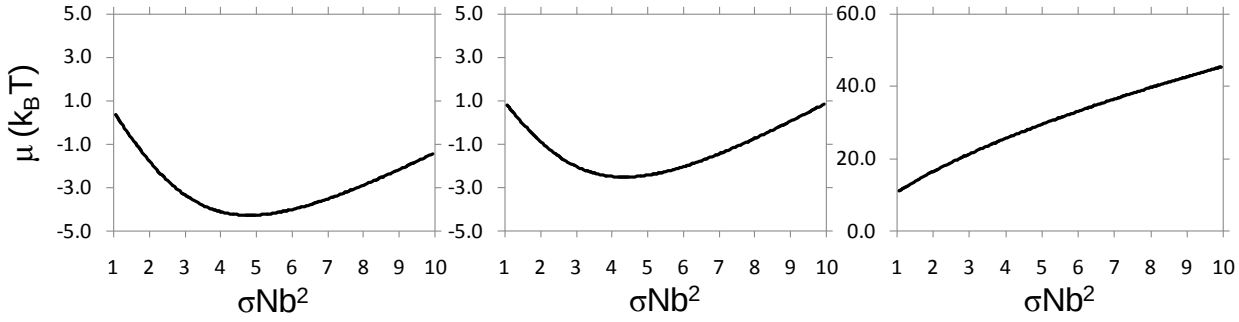

Figure S13. Plots of the polyelectrolyte chemical potential (μ) as a function of σ for strong (or quenched) polyelectrolyte brushes, calculated according to Equation (8) with three different fixed values of the fraction of charged monomers (f = 0.05, 0.10 and 0.50), under seven different salt conditions, i.e., (A) 0, (B) 20, (C) 60, (D) 80, (E) 100, (F) 300 and (G) 500 mM NaCl. The parameter values used are N = 100 (chain length), b = 7 Å (monomer size), v = 0 Å^3 (excluded volume), $w = 10^4$ Å^6 (three-body interaction coefficient), $C_{H_3O^+} = 10^{-7}$ M (bulk hydronium ion concentration), and $\sigma = 3Nb^2$ (grafting density). Note that here the solvent is assumed to be a θ solvent (i.e., v = 0).

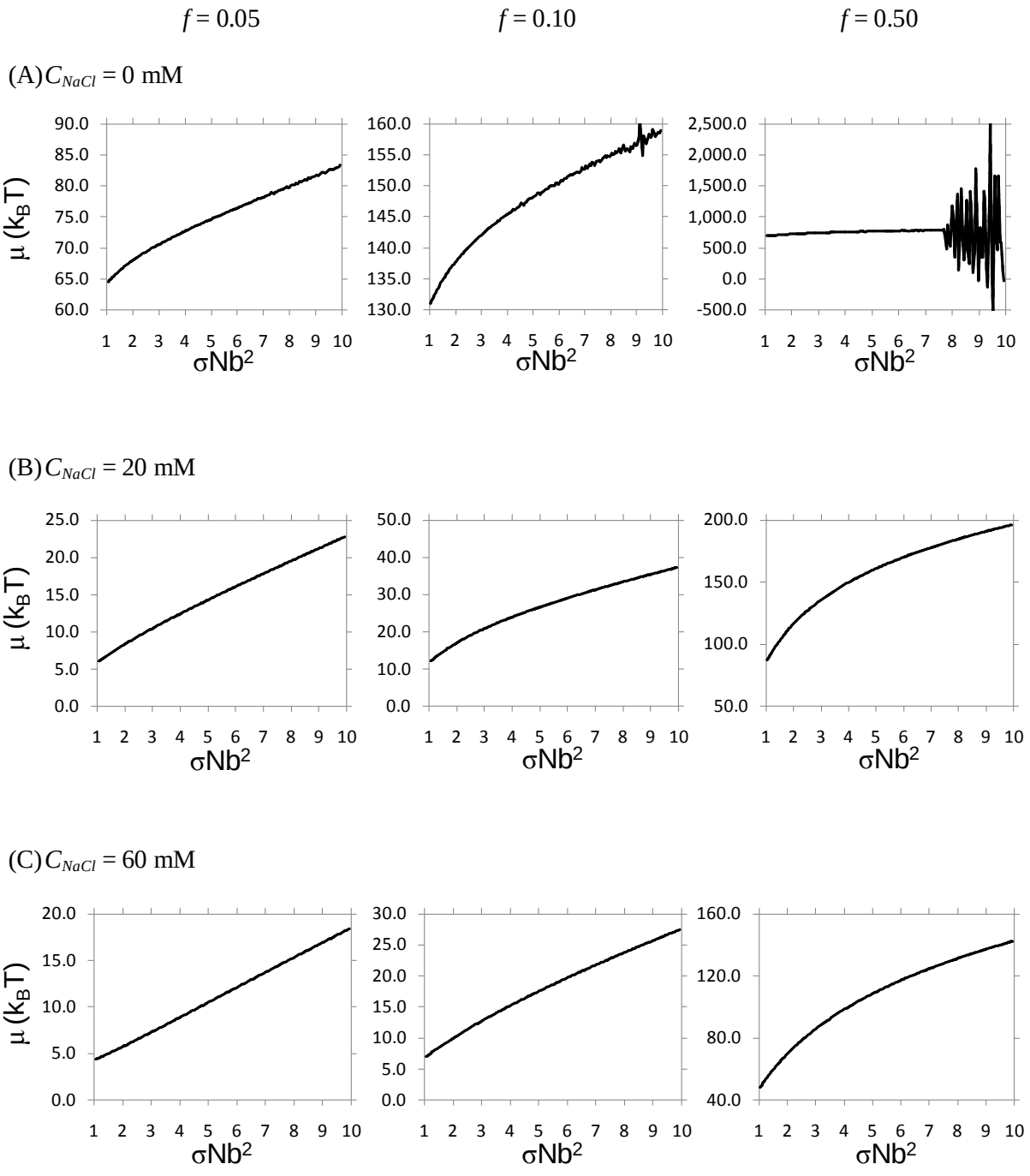

(D) C_{NaCl} = 80 mM

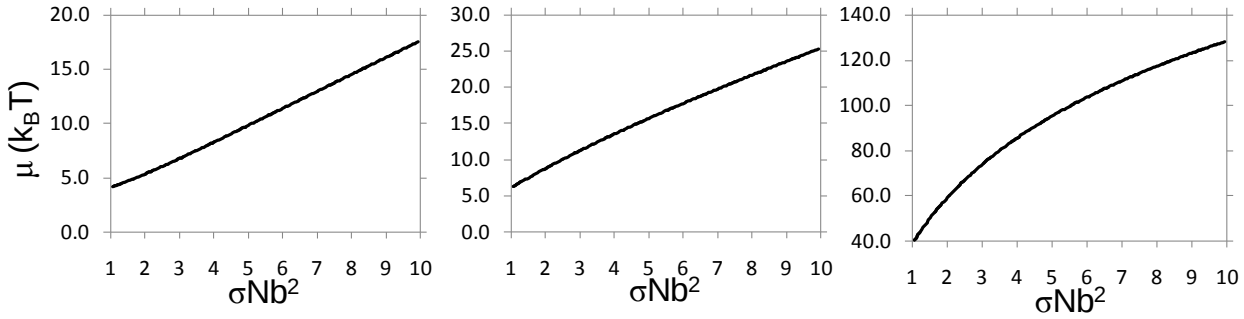

(E) C_{NaCl} = 100 mM

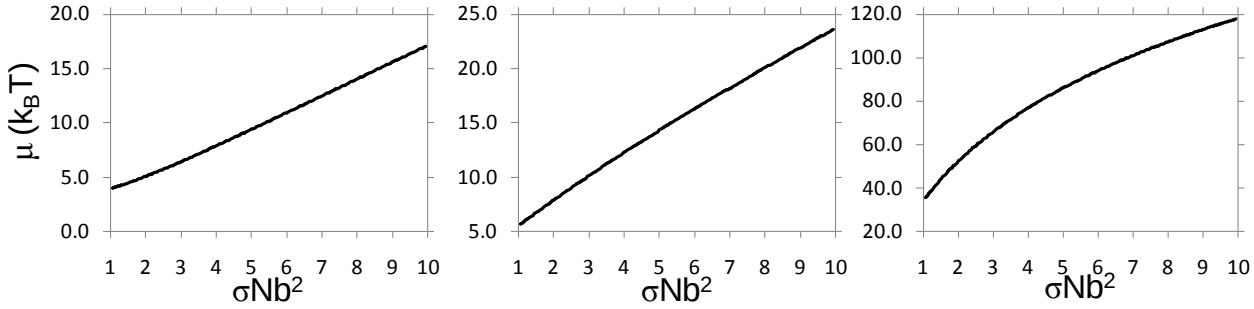

(F) C_{NaCl} = 300 mM

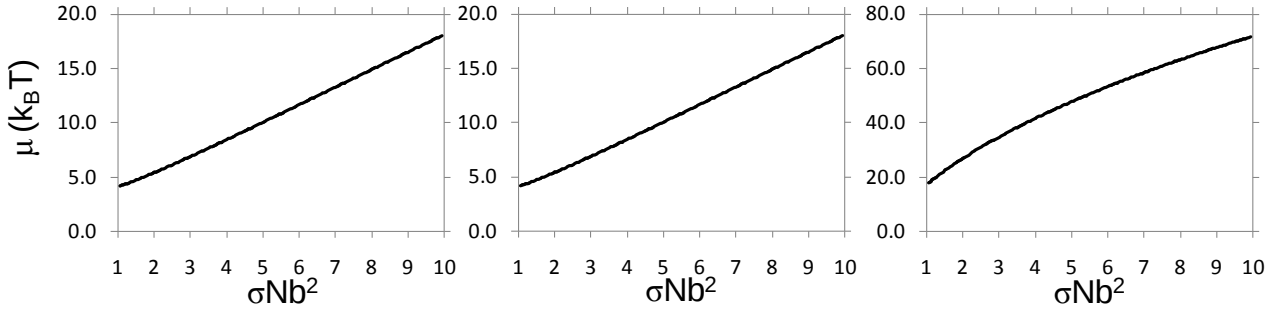

(G) C_{NaCl} = 500 mM

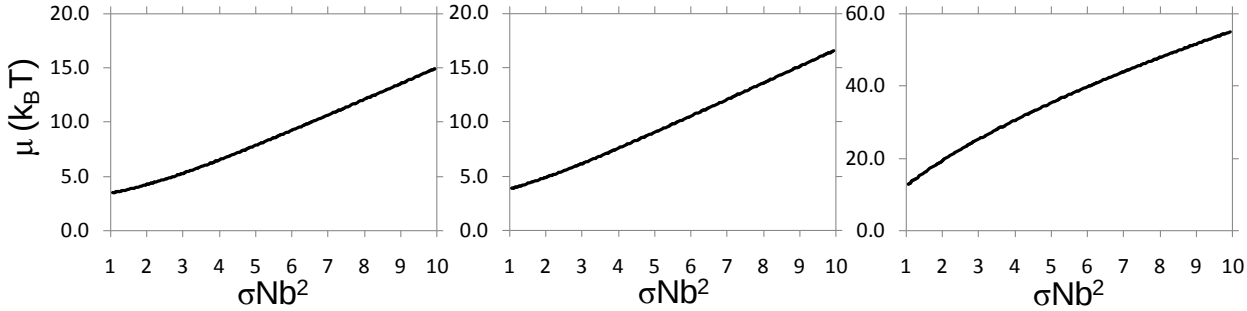

Table S1. Measured pH values and NaCl concentrations in the subphase solutions collected from the PDMAEMA-PnBA Langmuir monolayer systems used for the preparation of the gradient brush AFM specimens. These measured pH and conductivity values of the subphase solutions were invariant (within measurement error) for a tested period of a month, i.e., from immediately after to one month after the preparation of the subphase samples; after collection, the subphase solutions were stored in glass vials sealed with polyethylene plug caps. We did not use a pH buffer to stabilize the pH of the subphase solutions. We speculate that during the LB\C AFM sample preparation process (which typically took several hours) all chemical reactions in the subphase solutions (i.e., the protonation of PDMAEMA, and the dissolution and reaction of CO_2 with water) had already reached equilibrium, and therefore the pH and conductivity values of the subphase samples collected after the LB\C process did not change over time afterwards. The pH measurements were conducted using an Orion 420A Plus pH meter with proper cleaning and calibration of the instrument prior to each measurement. The conductivities were measured using a commercial conductivity meter (YSI Model 3200) following the procedures suggested by the manufacturer. Of note in the data below, the pH of the subphase solution was found to be a slightly decreasing function of NaCl concentration. In our theoretical analysis (Section 3.3), however, we did not include this small variation of pH with ionic strength; we examined the thermodynamic stability of the brush system at various NaCl concentrations, assuming, for simplicity, a constant pH of 7 for all salt concentrations. The incorporation of the observed pH variation into the calculation does not yield results (qualitatively) different from those presented in Section 3.3.

Concentration of added NaCl (mM)	pH	Conductivity (μS/cm)	NaCl concentration estimated from conductivity (mM)	Temperature (°C)
0	7.25 ± 0.04	0.93 ± 0.01	0.0182 ± 0.0002	22.3
20	7.17 ± 0.03	1090 ± 20	21.4 ± 0.4	23.1
60	7.05 ± 0.05	3070 ± 30	60.2 ± 0.6	22.1
80	6.97 ± 0.03	4100 ± 30	80.4 ± 0.6	22.5
500	6.85 ± 0.04	25800 ± 280	505.9 ± 5.5	21.9

Table S2. Values of the degree of monomer protonation (f) and the local pH of the solution within the brush layer estimated using Equations (2) and (3) of the main text for various concentrations of added NaCl.

C_{NaCl} (mM)	f	$c_{H_3O^+}$ (Å^{-3})	pH in the brush layer
0	0.0019	4.463×10^{-15}	11.13
0.018	0.0247	6.074×10^{-14}	9.996
20	0.5545	2.984×10^{-12}	8.305
60	0.7358	6.678×10^{-12}	7.955
80	0.7773	8.369×10^{-12}	7.857
100	0.8066	9.998×10^{-12}	7.780
300	0.9068	2.332×10^{-11}	7.412
500	0.9303	3.199×10^{-11}	7.275